

Correlations of triggering noise in driven magnetic clusters

Bosiljka Tadić*

Jožef Stefan Institute, P.O. Box 3000, 1001 Ljubljana, Slovenia

We show that the temporal fluctuations $\Delta H(t)$ of the threshold driving field $H(t)$, which triggers an avalanche in slowly driven disordered ferromagnets with many domains, exhibit long-range correlations in space and time. The probability distribution of the distance between *successive* avalanches as well as the distribution of trapping times of domain wall at a given point in space have fractal properties with the universal scaling exponents. We show how these correlations are related to the scaling behavior of Barkhausen avalanches occurring by magnetization reversal. We also suggest a transport equation which takes into account the observed noise correlations.

I. INTRODUCTION

Field driven disordered ferromagnets at low temperatures exhibit Barkhausen (BH) noise, a very important physical phenomenon, which is used for noninvasive characterization technique in commercial alloys. It has been recognized that measured BH noise exhibits scale free behavior when only the external field is varied for all values of disorder and driving fields in real experiments [1–4] (a short summary of the experimental data can be found in Ref. [5]). This is in sharp contrast to some theoretical conclusions [6] emphasizing fine tuning of the strength of disorder to a single critical value. It has been also attempted to understand the dynamics of domain walls which results in BH avalanches in terms of the dynamics of a sandpile model [7,8] (for a recent review of sandpile models see [9]) and of the models of interface depinning [3,10–12]. It should be stressed that in BH noise the presence of disorder plays an important role via pinning of domain walls. It remains to be understood how the motion of domain walls is affected by the pinning.

Different scaling behaviors of BH noise can be attributed to the domain structure, which is related to annealing and type of impurities, and nucleation and coalescence of domains, as well as a varying driving conditions. Annealing the samples in the applied anisotropic stress or in the magnetic field leads to a characteristic structure of extended system-size domains with a 180° domain walls parallel to the anisotropy axis [13,10,11]. Numerical simulations with extended domain wall in two dimensions [12] led to the conclusion that different scaling behavior can be expected in two limiting cases: (a) When disorder is weak BH response is dominated by motion of a single (extended) domain wall; (b) For strong disorder a multidomain structure occurs with many competing domain walls. This picture is in a qualitative agreement with experimental results in stress annealed Fe-B-Si [10] and Fe-Co-B [11] alloys. Therefore the two different universality classes can be related to surface and bulk criticality, respectively. Numerical simulations starting from a uniform ground state [6,14,15], on the other hand, do not take into account extended domain walls, and thus cor-

respond to the behavior at high-disorder. In both cases, however, the origin of scaling has not been fully understood.

Recently the exact results of the random-field Ising model on the Bethe lattice [16] show that the avalanche distributions at a fixed driving field have finite cutoffs. However, an infinite cutoff appears for a range of disorder strengths $\Delta < \Delta_c$ if a distribution is integrated over the hysteresis loop. The integration thus involves an infinite jump in magnetization (when system size $L \rightarrow \infty$) at a critical value of driving field. On the other hand, for strong disorder Δ above Δ_c the avalanche distributions remain exponentially damped for all fields [16]. These results encourage further study of the field-integrated distributions to elucidate the role of driving field in the appearance of the scale-free BH noise.

In this work we study properties of the threshold driving field which triggers Barkhausen avalanches in the multidomain structure, which is generated in the linear part of the ascending branch of hysteresis. When the system is slowly driven by increasing the external magnetic field H with time, even by continuous field changes, there exists a *threshold* field that equals weakest pinning force of a domain wall in the system and thus starts an avalanche. In the numerical experiment we can adjust the driving field updates to the weakest local field in a system (so-called infinitely slow driving), and thus we can examine precisely the properties of the triggering noise. Surprisingly, we find that time series of such field updates are long-range correlated. Both Fourier spectrum of the threshold field fluctuations $\Delta H(t) \equiv H(t+1) - H(t)$ and distribution of distances of the successive avalanches which that field triggers appear to decay with a power law. The exponents are (weakly) universal in a range of values of disorder where BH avalanches have a power-law distributions. In addition, we find that the distribution of trapping times of domain wall at a given point in space exhibits scaling behavior. We show how the long-range noise correlations and fractal properties of the trapping time distribution are related to the observed scaling behavior of BH avalanches.

The present study is motivated by recently observed pattern formation [17] and activity correlations along a

driven interface [18–20] in 1 + 1 dimensions stacked by random defects. In contrast to these models, here we have a 2-dimensional system with many interacting interfaces, and two separate time scales (compared to extremal driving): slow time scale of field updates, and avalanche propagation time scale between two field updates. Despite of these differences, in both cases the intermittent avalanche-like dynamics occurs, which we believe is essential for the observed scaling behavior.

II. MODEL AND SIMULATIONS

We consider a simple model with disorder represented by local random fields h_x , which appears from an original disorder via coarse-graining

$$\mathcal{H} = - \sum_{\langle x, x' \rangle} J_{x, x'} S_x S_{x'} - \sum_x (h_x + H) S_x, \quad (1)$$

where $x \equiv (x_{\parallel}, x_{\perp})$ and $J_{x, x'} = 1$ is a constant interaction between nearest-neighbor spins $S_x = \pm 1$. A Gaussian distribution of h_x is assumed with zero mean and width f . (Other types of disorder have been also considered [5,14,15]). A domain wall of reversed spins is created along $\langle 11 \rangle$ direction [21] on the square lattice rotated by $\pi/4$. This model is motivated by the extended domain walls in stress-annealed samples, as discussed in Ref. [12]. Periodic boundaries are applied in the direction of wall and an open boundary at the opposite side of the wall. The system is driven *globally*—updated value of the external field is applied to all spins in the system. The dynamics consists of spin flips when the local field exceeds zero (see below).

As discussed in Ref. [12], the fact that motion of the $\langle 11 \rangle$ domain wall has no energy threshold at vanishing disorder has several advantages. In particular, the wall depinning occurs along a line $H_c(f) \sim \kappa f$ in the (f, H) plane, where κ is a constant (see Fig. 2 in Ref. [12]). Therefore for the domain wall along $\langle 11 \rangle$ direction an *infinitesimally small* field H is sufficient to move and depin the domain wall for small disorder, $H_c(f) \rightarrow 0$ for $f \rightarrow 0$. This important property of the model allows us to use much smaller lattice sizes compared to earlier studies [22,6], where a large system has to be used in order to find a random field large enough to surmount the energy barrier $2J$ in the case of wall along $\langle 10 \rangle$ direction, or the nucleation energy $4J$ in the case of uniform ground states. On the other hand, by increasing disorder the distance between pinning centers decreases, and thus a critical disorder f^* exists at which depinning is no longer possible. Instead, it becomes energetically easier to nucleate new domains in the bulk. The exact value of f^* depends on the type of distribution [12,16], and is still not known exactly. In Ref. [12] it was found using a finite-size scaling analysis of the averaged interface velocity and avalanche distributions that for the present model $f^* = 0.62$ within numerical error bars.

The scaling properties of BH avalanches in low disorder regime were discussed in Ref. [12]. Here we are interested in the high disorder region, where the $\langle 11 \rangle$ interface remains pinned at all fields. Nevertheless, the initial state with the $\langle 11 \rangle$ interface ensures that the ratio of the characteristic lengths $\xi_1/L \ll 1$ holds for the applied disorder values (thus the avalanche size cut-off $s_0 \ll L^2$). (The characteristic length ξ_1 represents distance between strong pinning centers [22] for given strength of disorder.) On the contrary, when $\xi_1/L \sim 1$, the $\langle 11 \rangle$ interface moves, meaning that the selected system size L is small for given strength of pinning, and thus system is not in the high disorder regime. Thus, having the condition $\xi_1/L \ll 1$ satisfied for each applied value of disorder, we can concentrate on the effects of disorder fluctuations by applying many configurations of random fields at fixed f and L values. We use up to $L = 768$ and up to 10^3 disorder configurations (i.e., up to 36×10^6 spins).

Since we are interested in the properties of the triggering noise, which are related to distribution of disorder and the actual dynamics of the system, we avoid any “short-cuts” which can speed the algorithm [24]. We apply the natural slow algorithm, which consists of the following steps: Random fields are stored at each site of an $L \times L$ lattice; The system is searched for the minimum local field $h_{min} = \min(h_x^{loc})$, where $h_x^{loc} \equiv \sum_{x'} J_{x, x'} S_{x'} + h_x + H \equiv h_{ir, x} + H$, and then the driving field is set to exactly $h_{min} + \eta$ (we use $\eta = 10^{-10}$), which thus triggers an avalanche at that site; A list is made consisting of the sites which may flip at the next time step (neighbor sites to flipped spins); The spins on the list are examined for flip and a new list is made; The process is continued until no more spins can flip, then next minimum local field is found. It should be stressed that all spins in a single list (spin shell) are updated in parallel, i.e., in a single time step, in analogy to parallel update in cellular automata models. In this way we have well defined time scale of avalanche evolution (internal time scale) as the number of steps that the updating procedure goes before the avalanche stops. On the other hand, the slow (external) time scale is set by the number of driving field updates.

It was shown in Ref. [12] that for low disorder $f < f^* = 0.62$ the extended domain wall moves through the system and depinns at a critical field $H_c(f)$, however, above the critical disorder f^* the built-in domain wall remains pinned and many new domains of reversed spins are nucleated inside the system. In this region, corresponding to high disorder (or low tensile stress), a typical structure of clusters which occurs in the linear part of the hysteresis is shown in Fig. 1. The theoretical value f^* can, in principle, be related to a critical value of tensile stress $\sigma^* \sim f^{*\mu}$, below which the domain structure changes, as also observed in the experiment in Ref. [10]. More precise experimental data would be necessary in order to determine the exponent μ . A rough estimate is that μ is given by the correlation length exponent at the transition f^* , $\mu \approx \nu \sim 2.3$ [12].

III. FRACTAL PROPERTIES OF TRIGGERING NOISE AND DOMAIN-WALL TRAPPING

Time series of the magnetization jumps corresponding to the individual avalanches are known as BH noise. In the high disorder region either a new domain is nucleated and grown, or already existing domain extended, a BH pulse is associated with motion of a domain wall from one position to a new one. The area between two consecutive domain wall positions corresponds to the size of BH avalanche (measured as the area covered by a single BH pulse). In principle, a domain growth process is not “linear” but fractal, leading to the dynamic exponent $z = 1.23$, and fractal dimension of avalanche $D = 1.88$ [12]. As usual, the dynamic exponent z and the fractal dimension D are defined via the scaling of characteristic duration and size of avalanches with the change of length scale, $\langle t \rangle_L \sim L^z$, and $\langle s \rangle_L \sim L^D$, respectively. Scaling properties are studied in detail (see set of scaling exponents in Ref. [12]). In particular, in the critical region above f^* the distribution of size of avalanches $D(s) \sim s^{-\tau_s}$ and duration $P(t) \sim t^{-\tau_t}$ scale with the exponents $\tau_s = 1.30$ and $\tau_t = 1.47$, respectively. The avalanche distributions integrated over hysteresis loop for $f > f^*$ can be scaled according to the scaling form [12]

$$P(t, f, L) = t^{-\tau_t} \mathcal{P}(t(\delta f)^{z\nu}, tL^{-z}), \quad (2)$$

where $\delta f \equiv (f/f^* - 1)$ and $(\delta f)^{-\nu}$ measures the correlation length due to the critical point at f^* . For instance, when the condition $L \gg (\delta f)^{-\nu}$ is satisfied, the avalanche cut-offs can be scaled with disorder strength (*in the entire region of power-law behavior*), leading to $f^* = 0.62$ and $\nu = 2.3$ within statistical error bars (see [12] for details). It should be stressed that in this region of disorder the spatial extension of an avalanche is determined not only by strength of pinning but also by the blocking by previous clusters (see Fig. 1). The blocking effects dynamically alter the strength of pinning and thus influence the scaling properties. This illustrates a complex interplay between the disorder and dynamics, in contrast to, for instance, the equilibrium clusters in the random-field Ising model. In order to get an insight into these complex phenomena, we study next the distributions of wall trapping times and distances between the points with weakest pinning, from which an avalanche is released. We find that both of these distributions exhibit a scaling behavior.

The distribution of distances between initial points of the *successive* avalanches is shown in Fig. 2, where we distinguish between distances measured in the parallel (x_{\parallel}) and transverse (x_{\perp}) direction relative to the direction of the wall. In fact, due to anisotropy of domain wall motion in this case, these distributions show different scaling exponents $\tau_{\parallel} = 1.04 \pm 0.03$ and $\tau_{\perp} = 0.60 \pm 0.03$ according to

$$G(x_{\parallel}, x_{\perp}) \sim x_{\parallel}^{-\tau_{\parallel}} \mathcal{G}(x_{\perp}/x_{\parallel}^{\zeta_G}), \quad (3)$$

where $\zeta_G = \tau_{\parallel}/\tau_{\perp}$. Notice that for small distances correlations in both directions are almost equivalent. However, a crossover to a distinct power-law behavior for $G(x_{\perp})$ occurs at a distance ($x \approx 30$ in Fig. 2) which is presumably related to the characteristic size of avalanche at given disorder. The open boundary in the direction opposite to wall leads to the cut-off at large x_{\perp} . It should be stressed that spatial correlations are sensitive to distribution of disorder. Therefore, here we used a large number of samples in order to minimize scatter of the data due to disorder fluctuations and to clearly distinguish between correlations in parallel and perpendicular directions.

In the inset to Fig. 2 we show the Fourier spectrum of the threshold field fluctuations $\Delta H(t)$ measured on the external time scale. It exhibits two correlated regions corresponding to earlier and later times, respectively. Steeper slope in the inset to Fig. 2 vary from 0.6-1.03, and flatter slope from 0.25 to 0.36, depending on f . The long-range correlations exhibited in Fig. 1 show that the system evolves in such way that its next relaxation event depends on the history of the present state of the system. It is interesting to note that a similar time series of the fluctuation of magnetization $\Delta M(t) \equiv M(t+1) - M(t)$ represents the Barkhausen noise itself (looked at the external time scale). An example of the BH noise signal is shown in Fig. 3. Note that on the external time scale duration of each elementary signal is equal to one, whereas the height of each elementary signal represents corresponding avalanche size. Sizes of the successive avalanches are only weakly correlated in time. However, a time *derivative* of the signal, namely $a(t) \equiv d[\Delta M(t)]/dt$, representing acceleration of a domain wall at each field update, shows certain correlation properties. In the inset to Fig. 3 we show the Fourier spectrum of the numerical derivative of the signal, which is shown in main Fig. 3. Average slope of the curve is close to one.

It should be noted that the average number of avalanches occurring at fixed strength of disorder increases with system size as $\langle n_a \rangle \sim L^2/\langle s \rangle \sim L^{[2-D(2-\tau_s)]} \phi(L(\delta f)^{\nu})$, where $\phi(L(\delta f)^{\nu})$ is unknown scaling function. This implies that in the theoretical case of infinitely slow driving the average size of the field jump $\langle \Delta H(t) \rangle$ decreases with L as $\langle \Delta H(t) \rangle \sim H_{sat}(L)/\langle n_a \rangle \sim L^{-0.68} H_{sat}(L)/\phi(L(\delta f)^{\nu})$, where H_{sat} is the saturation field. In real experiments the size of field jumps are restricted by the driving frequency, however, number of avalanches detected varies with the size of pick-up coil. This problem requires more detailed theoretical and experimental investigation [25].

Further understanding of the role of disorder in the dynamics can be achieved by considering the time intervals that a domain wall resides at a given point in space (trapping time T_{trap}). We calculate the distribution of trapping times T_{trap} of a domain wall at a given site,

which is determined as the time interval since the domain wall is pinned at a site $(x_{\parallel}, x_{\perp})$ until it eventually moves away from that site. In this way, T_{trap} measures the time interval between two successive activities at that site. Notice that T_{trap} in this case is somewhat different from so called first-return time in 1-dimensional interface [18]. Here we have 2-dimensional system with many interacting interfaces. Another similar example is trapping of grains in rice-pile models [26]. A reasonable time scale to measure T_{trap} is the number of field updates (external time scale), since in the zero-temperature dynamics during an avalanche a spin at a given site is either fixed or flips only once.

The trapping-time distribution is shown in the inset to Fig. 4 for various values of disorder $f > f^*$. Between the lower cut-off T_0 (below which all trapping times are equally probable), and an upper cut-off due to lattice size L , the trapping time distribution shows a short region with correlations. In particular, for large trapping times we can determine the slope as $\tau_{trap} = 2.3 \pm 0.1$. One can understand that a metastable configuration of domain walls corresponds to the system residing in a ‘‘pocket’’ of the fractal free energy landscape. A domain wall may move from a site $(x_{\parallel}, x_{\perp})$ as a part of an avalanche which started in the neighborhood of that point, corresponding to a local reorganization of the landscape near a shallow minimum (for a given value of the external field). When the system resides in a deeper minimum, however, it waits for larger driving fields (*i.e.*, trapping time increases) or for a more global reconstruction of the landscape, which occurs with smaller probability compared to the one discussed above. This leads to the large slope of the distribution $P(T_{trap}) \sim T_{trap}^{-\tau_{trap}}$ at large T_{trap} . It is interesting to note that a similar slope for large trapping times was found in the case of rice-pile model [26], where trapping of grains are considered, and it was argued that the slope is related to the roughness exponent of the rice-pile surface (see detailed analysis in Ref. [26]). Analogies between an interface motion and rice-pile model have been established in the literature [27]. Considering the avalanche exponents the analogy also applies for the BH noise with an extended domain wall in the limit of low disorder [12]. Notice that, in contrast to ricepile model, the range of power-law behavior in BH noise depends not only on the system size, but also on the strength of disorder, which restricts spatial extension of avalanches to $s \leq s_{max} \ll L^2$ and their durations to $T \leq T_{max}$. Therefore, in this region of disorder we have rather small range of the power-law behavior. However, the scale-free behavior of the distribution of trapping times can be demonstrated via finite size scaling analysis when different system sizes are used. We find that the following scaling form

$$P(T_{trap}, L) = L^{\alpha} \mathcal{P}(T_{trap} L^{-z_T}), \quad (4)$$

applies with the exponents which are weakly dependent on disorder $\alpha = -0.4 \pm 0.05$ and $z_T = 1.66 \pm 0.05$ (see Fig.

4). By increasing the system size L the trapping times increase, leading to larger cut-offs of the distribution. We notice that the lower cut-offs T_0 also increase, leaving a limited correlation range. However, the cut-offs scale nicely with L , as shown in Fig. 4. In the inset to Fig. 4 we show how the trapping times distribution varies with disorder. By increasing disorder the cut-off T_0 moves towards larger values and the correlation region shrinks, corresponding to a lesser correlations in the dynamics, which also manifests in the decrease of the characteristic avalanche size. In the limit of infinitely strong disorder the dynamics becomes completely random, consisting of individual spin flips which align along a local random field.

It is interesting to note that unlike the avalanche distributions in Eq. (2), the distribution of trapping times in Eq. (4) as well as $G(x)$ (3) do not show explicit disorder dependence apart from a weak dependence in the exponents. In fact, the disorder effects in this case are included in the gradient of driving force ΔF (*i.e.*, the increments of the external field ΔH , which are adjusted to the minimum local fields). For example, for the distribution of trapping times we have in general

$$P(T_{trap}, L, \Delta F) = L^{\alpha} \mathcal{P}(T_{trap} (\Delta F)^{z_T/\lambda_F}, T_{trap} L^{-z_T}), \quad (5)$$

where the increase in the driving force $\Delta F \equiv H(t + T_{trap}) - H(t)$ contains all the contributions due to interaction and random pinning which occurred during the time interval $(t, t + T_{trap})$, *i.e.*, $\Delta F = \sum_t^{t+T_{trap}} h_{ir,x}$, which steam from the different sites in the system. According to the above results in Fig. 2, sum of these contributions has no characteristic scale. Therefore we may conclude that $(\Delta F)^{-1/\lambda_F} \rightarrow \infty$. Hence the first argument in the right hand side of Eq. (5) can be neglected compared to $T_{trap}/L^{z_{trap}}$, leading to the scaling form (4), which is in agreement with the scaling plot in Fig. 4.

Another interesting observation regards the dynamic exponent z_T , which scales the tail of the trapping time distribution with the system size L . It may be related to the scaling of the length of the optimal path [29] in strongly disordered medium, $z_T = D_{OP}$. In fact, the optimal path between two points can be constructed from the *most persistent sections* of the domain walls in the dynamics of BH avalanches. The length of the optimal path scales with the linear distance between the end points with the exponent $D_{OP} = \tau_{OP} = 1.66$ [28,29].

IV. TRANSPORT EQUATION WITH NOISE CORRELATIONS

The long-range noise correlations are shown to be relevant for the scaling properties of the interface motion [30]. In the literature the noise correlations in the interface depinning are viewed as originating from another (external) dynamic processes [30]. In the case of

Barkhausen avalanches we see that the noise correlations appear as an intrinsic property of the dynamics when the system is driven infinitely slowly. The active section of domain wall can be represented by a surface $h(x, \tau)$ which is pinned by quenched defects. The transport at the site (x, τ) is described by the equation

$$dh/d\tau = \nu_{\parallel} \partial_{\parallel}^2 h + \nu_{\perp} \partial_{\perp}^2 h + \eta(x, t, h). \quad (6)$$

Here we distinguish total elapsed time τ , which is defined as the sum of evolution times of all individual avalanches, on one hand, and t , which represents time scale of field updates, on the other. The quenched noise $\eta(x, t, h)$ is generated by varying the driving field in the steps which are adjusted to the minimum local strength of pinning, as discussed above. We expect that a dominant h -dependence of the noise η can be expressed as $\eta \sim p(x) \partial h$, where $p(x)$ represents the (anisotropic) local velocity of domain wall per field rate. In addition, time variation of the noise are related to the updates of the external field, and thus η varies on the external time scale only. Therefore, we can write

$$\eta(x, t, h) \approx p(x)(a_0 + \Delta H(t))(\partial h), \quad (7)$$

where a_0 is a constant which depends on initial configuration and the hysteresis loop properties. The local interface velocity per field rate, $p(x)$, is a random variable which is determined by the spatial distribution and strength of pinning associated with a given value of the driving field H , i.e., history of the system. Therefore $p(x)$ is governed by a probability distribution, which can be deduced from the properties of the probability that an avalanche starts at distance x from the preceding avalanche, i.e.,

$$\langle p(x)p(x') \rangle = \gamma G(x - x'). \quad (8)$$

It is assumed that the same type of correlations apply for the successive activities during the evolution of an avalanche, while the external field is constant. In the previous section we found that the probability $G(x)$ exhibits long-range correlations in the perpendicular and parallel direction as $G(x_{\parallel}, x_{\perp}) \sim x_{\parallel}^{-1} x_{\perp}^{-0.60}$. We also notice that $\Delta H(t) \sim t^{-\theta}$, where θ is finite in the case of infinitely slow driving discussed above, whereas, $\theta = 0$ in the case of finite driving rate in small steps [15], where $\Delta H(t) = \text{const}$. Notice that Eq. (6) together with Eqs. (7) and (8) leads to an effective nonlinear term of the form $\gamma G(x_{\parallel}, x_{\perp})(a_0 + t^{-\theta})^2 (\partial h)^2$, which differs from the Kardar-Parisi-Zhang nonlinearity [31] by the power-law correlations in the coefficient. As discussed above, the origin of these correlations lies in the the dynamically varying pinning and blocking effects when a multidomain structure is slowly driven through the hysteresis loop.

The relevance of the noise correlations for the universality class of the interface depinning has been discussed in the literature using dynamic renormalization group (RG) [30]. Another example where correlations

of random noise play an important role is represented by the scaling properties of river networks [28,32]. In that case the correlations of the type $G \sim x_{\parallel}^{-2+\delta} x_{\perp}^{1-\zeta}$ were assumed, where δ is an expansion parameter and the anisotropy exponent ζ has to be determined self-consistently at a fixed point of the RG [28]. In the result, the scaling exponents do depend on the range of correlations δ . Similarly, we can expect that the long-range correlations of the form given in Eqs. (7) and (8) can be related to the universal scaling exponents of the BH noise. The exponents z , ζ_G , which are defined above, and the roughness exponent χ , which governs behavior of the dynamic variable h with the change of scale, can in principle be obtained by the dynamic RG applied to Eq. (6) with noise properties in Eqs. (7-8). Then the avalanche exponents τ_t and τ_s can be deduced using scaling relations in the critical region. The RG analysis of the transport equation (6) with noise properties specified by Eqs. (7-8) requires additional work and is left out of the scope of this paper. Here we discuss only the scaling relations between the exponents at RG fixed point, e.g., the dynamic exponent z , and the avalanche exponents.

It should be stressed that such scaling relations are not universal and that they depend on the nature of the dynamic process (see for instance [28,32] for the case of river networks). We argue that the scaling relation derived below are valid for BH avalanches in the high-disorder (or multidomain) region. The rationale behind these scaling relations is found in the directed nature of the avalanche propagation. The evolution of an avalanche (see Fig. 1) can be visualized as growth of a directed percolation (DP) cluster projected [33] to 1+1 dimensions, with extra dimension representing time axis. The fractal dimension of the equivalent DP cluster measured with respect to the time axis is then $D_{\parallel} \equiv D/z$, where D and z are fractal dimension of BH avalanche and dynamic exponent, respectively, as defined above. Then $D_{\parallel} = 1 + \zeta_{DP} - \delta_{DP}$, where $\zeta_{DP} = z/2$ is the anisotropy exponent measured with respect to time axis, and δ_{DP} is the survival probability exponent of the equivalent DP clusters. Notice also that for the directed dynamic processes $\tau_t = D_{\parallel}$ and thus $\tau_s = 2 - 1/\tau_t$ [34], which completes the set of avalanche exponents. In addition, the roughness exponent χ can be related to the trapping time distribution as $\tau_{trap} = 2 + \chi$, as noticed in Refs. [26,27]. For instance, using the numerical values for D and z from Ref. [12], the following values of the avalanche exponents are predicted by the above scaling relations: $\tau_t = 1.52$, $\tau_s = 1.34$, compared with 1.47 and 1.30, and $\chi = 0.23$, obtained by direct numerical simulations.

V. CONCLUSIONS AND DISCUSSIONS

We have demonstrated numerically the existence of long-range correlations in triggering noise which is intrinsic to the domain wall dynamics in slowly driven dis-

ordered ferromagnets. Although the distribution of disorder is initially uncorrelated, the spatio-temporal correlations develop in time. The appearance of these correlations can be attributed to the applied global driving in which always *next weakest* pinning force in the system is selected, on one hand, and to a finite extension of avalanches occurring between two consecutive field updates, on the other. Hence, attempts to reduce the domain wall dynamics to the Glauber spin flips in the presence of local random fields appears to be inadequate for the range of disorder where the cooperative avalanche dynamics occurs. We suggest an alternative transport equation which incorporates the observed noise correlations. The long-range correlations of triggering noise can be related to the universal scaling behavior of Barkhausen avalanches and to the transport properties *via* the fractal distribution of the domain wall trapping times. We believe that an analysis of the transport equation by the dynamic RG will contribute to understanding of the universality classes of Barkhausen avalanches by the infinitely slow driving. By varying the driving conditions, however, these correlations are changed. This might be the origin of different scaling behavior of BH avalanches at finite driving rates, as observed in experiments [11]. Our results also suggest that technical procedures which speed the numeric algorithms in driven disordered systems should be taken with care. In particular, an algorithm which alters the properties of triggering noise may lead to a different scaling behavior, which is unrelated with the original problem.

ACKNOWLEDGMENTS

This work was supported by the Ministry of Science and Technology of the Republic of Slovenia. I am grateful to Deepak Dhar for many helpful comments and suggestions.

* Electronic address: Bosiljka.Tadic@ijs.si

- [1] L.V. Meisel and P.J. Cote, Phys. Rev. B **46**, 10822 (1992).
- [2] G. Bertotti, G. Durin, and A. Magni, J. Appl. Phys. **75**, 5490 (1994)
- [3] J. S. Urbach, R. C. Madison, and J. T. Markert, Phys. Rev. Lett. **75**, 276 (1995).
- [4] Dj. Spasojević *et al.*, Phys. Rev. E **54**, 2531 (1996).
- [5] B. Tadić, Physica A **270**, 125 (1999).
- [6] O. Perković *et al.*, Phys. Rev. Lett. **75**, 4528 (1995); e-print cond-mat/9807336
- [7] O. Geoffroy and J.L. Porttseil, J.Magn. Magn. Mat. **133**, 1 (1994).
- [8] A. Vásquez and O. Sotolongo-Costa, cond-mat/9903207.

- [9] D. Dhar, Physica A **263**, 4-25 (1999).
- [10] M. Bahiana *et al.*, Phys. Rev. E **59**,3884 (1999).
- [11] G. Durin and S. Zapperi, e-print cond-mat/9808224.
- [12] B. Tadić and U. Nowak, e-print cond-mat/9903090 and Phys. Rev. E (in press).
- [13] J. D. Livingston and W. G. Morris, J. Appl. Phys. **57**, 3555 (1985).
- [14] E. Vives and A. Planes, Phys. Rev. E **50**, 3839 (1994).
- [15] B. Tadić, Phys. Rev. Lett. **77**, 3843 (1996); Philosophical Mag. B **77**, 277 (1998).
- [16] S. Sabhapandit and D. Dhar, e-print cond-mat/9905236.
- [17] S. Krishnamurthy and M. Barma, Phys. Rev. Lett. **76**, 423 (1996).
- [18] K. Sneppen and M. H. Jensen, Phys. Rev. Lett. **71**, 101 (1993).
- [19] S. Roux and A. Hansen, J. Phys. I France **4**, 515 (1994).
- [20] M. Pazsusi, S. Maslov, and P. Bak, Phys. Rev. E **53**, 414 (1996).
- [21] A $\langle 11 \rangle$ interface was first introduced in U. Nowak and K.D. Usadel, Europhys. Lett. **44**, 634 (1998).
- [22] H. Ji and M. O. Robbins, Phys. Rev. A **44**, 2538 (1991).
- [23] I thank Sven Lübeck for providing the color map formula.
- [24] M. C. Kuntz *et al.*, e-print cond-mat/9809122.
- [25] Dj. Spasojević, private communication.
- [26] A. Corral, Ph. Thesis, unpublished; K. Christensen *et al.*, Phys. Rev. Lett. **77**, 107 (1996).
- [27] M. Pazsusi and S. Boettcher, Phys. Rev. Lett. **77**, 111 (1996).
- [28] B. Tadić, Phys. Rev. E **58**, 168 (1998).
- [29] M. Ceiplak *et al.* Phys. Rev. E (in press).
- [30] E. Medina, T. Hwa, and M. Kardar, Phys. Rev. A **39**, 3053 (1989).
- [31] M. Kardar, G. Parisi, and Y.C. Zhang, Phys. Rev. Lett. **56**, 889 (1986); L.-H. Tang, M. Kardar, and D. Dhar, Phys. Rev. Lett. **74**920 (1995).
- [32] J. R. Banavar *et al.*, Phys. Rev. Lett. **78**, 4522 (1997); A. Maritan *et al.*, Phys. Rev. E **53**, 1510 (1996).
- [33] Such projections are manifestly used in the problem of river networks [28,32].
- [34] B. Tadić and D. Dhar, Phys. Rev. Lett. **79**, 1519 (1997).



FIG. 1. Extended domain wall along the bottom line (shown in red), and unflipped spins (full blue color) and cluster of flipped spins developed at different stages of evolution (shown using a continuous color map [23]). Only 253 recent clusters are shown, with all older clusters shown in yellow color. $L = 200$ and $f=1.1$.

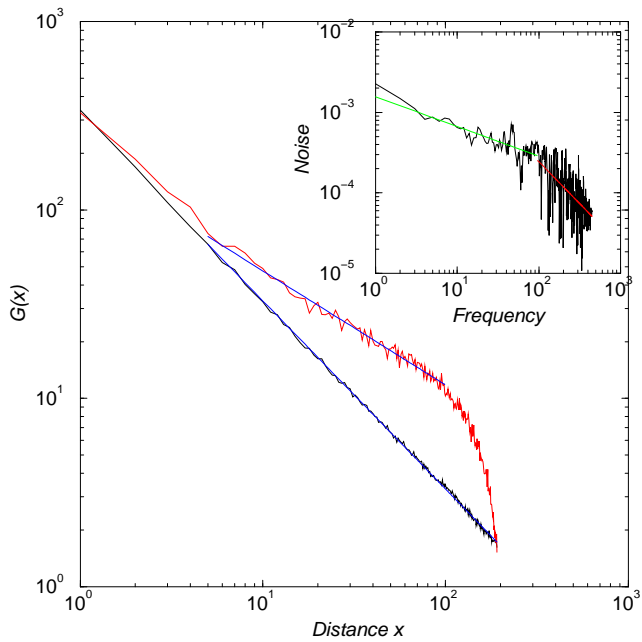


FIG. 2. The probability that the subsequent avalanche starts at the distance x_{\parallel}, x_{\perp} (bottom, top) from the point of the preceding avalanche for $L = 192$ and $f = 1.0$. The data are averaged over 1000 samples. Inset: Fourier spectrum of the driving field fluctuations $\Delta H(t)$ taken in *one* ascending branch of hysteresis for $f = 1.0$ and $L = 192$, vs. undimensional frequency.

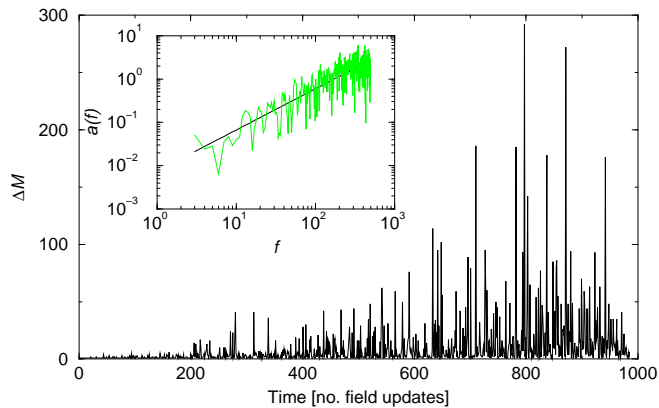


FIG. 3. Sequence of Barkhausen pulses ΔM (measured in number of spins) recorded on the time scale of field updates. Inset: Fourier spectrum of the numerical derivative of the sequence in the main figure plotted against undimensional frequency. Fitted slope is 0.95 ± 0.03 .

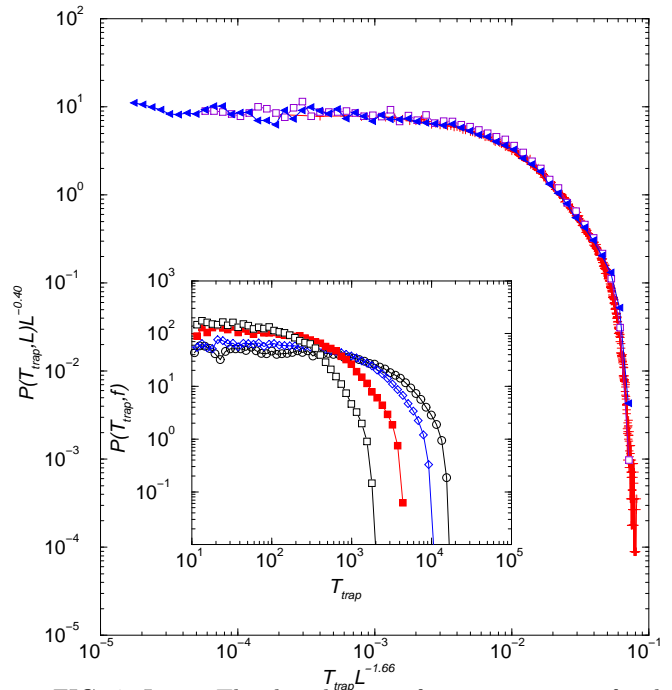


FIG. 4. Inset: The distribution of trapping times of a domain wall vs. trapping time T_{trap} measured by number of field updates. The distributions for various values of disorder $f=0.9, 1.0, 1.1,$ and 1.2 (left to right) are obtained at lattice 768×768 averaged over 10 samples. The data are logarithmically binned. Main: Finite size scaling plot of the trapping time distribution for $f=1.0$ and the linear lattice size $L=192, 384,$ and 768 . The data for $L = 192$ are averaged over 1000 samples, the rest of the data over 10 samples, and are logarithmically binned.